WPPFC-CPR(18) 18927

C Li et al.

Elemental Analysis on Wendelstein 7-X Limiter and Divertor Tiles by Laser-Induced Breakdown Spectroscopy (LIBS)

Preprint of Paper to be submitted for publication in Proceeding of 23rd International Conference on Plasma Surface Interactions in Controlled Fusion Devices (PSI-23)

This work has been carried out within the framework of the EUROfusion Consortium and has received funding from the Euratom research and training programme 2014-2018 under grant agreement No 633053. The views and opinions expressed herein do not necessarily reflect those of the European Commission.

Elemental Depth Analysis on Wendelstein 7-X Divertor Baffle Screws by Laser-Induced Breakdown Spectroscopy

Cong Li[1,2], Jannis Oelmann[2], Sebastijan Brezinsek[2], Marcin Rasinski[2], Chandra Prakash Dhard[3], Ralf König[3], Yunfeng Liang[2], Hongbin Ding[1], Christian Linsmeier[2] and the W7-X team[3]

[1]*Key Laboratory of Materials Modification by Laser, Ion and Electron Beams (Ministry of Education), School of Physics, Dalian University of Technology, 116024 Dalian, P. R. China*

[2]*Forschungszentrum Jülich GmbH, Institut für Energie- und Klimaforschung – Plasmaphysik, Partner of the Trilateral Euregio Cluster (TEC), 52425 Jülich, Germany*

[3]*Max-Planck-Institut für Plasmaphysik, 17491 Greifswald, Germany*

Abstract:

Analysis of elemental distributions in plasma-facing components (PFCs) is vital for the study of material erosion, deposition, and fuel retention in Wendelstein 7-X (W7-X) stellarator operating in full 3D geometry. In this work, a well-established composition analysis approach, laser-induced breakdown spectroscopy (LIBS), is employed to investigate the elemental depth distribution on screws with multilayer structure from the divertor baffle of W7-X in the first operational phase with passively cooled divertor (OP1.2a). A short pulsed laser system with pulse duration of 35 ps and wavelength of 355 nm is used to ablate the screws exposed in W7-X in an ultrahigh vacuum chamber. The screws are made of TZM – a molybdenum (Mo) alloy. A titanium (Ti) layer with about 1 μm thickness on top of the Mo alloy substrate, and protective carbon (C) layer with the thickness from 5.8 to 12.0 μm on top of the Ti layer. The accurate layer thicknesses are identified by focused ion beam (FIB) cutting. LIBS depth analysis clearly shows the hydrogen (H), C, Ti and Mo intensities depth profiles with the number of laser shots. In order to achieve the accuracy C thicknesses of the screws by LIBS, the linear correlation approach has been applied for improving the elemental depth profiles and identifying the interface between the C layer and the Ti layer. The correlation between the FIB thickness and the LIBS result are well fitted and shows that a LIBS ablation rate of (82.9 ± 0.9) nm/shot can be achieved on C layer thickness measurement by a laser energy density of 6.5 J/cm^2. In addition, H retention intensities on the surface of the screws with stellarator discharge plasma exposure at the baffle region of divertor in OP1.2a are higher than on the surface of the new screw without plasma exposure. The C-H deposition layer is found on the surface of exposed screws by scanning electron microscopy image. This indicates that the recessed screws located at the inboard side and outboard side baffles are representing net

deposition zones. The studies well demonstrate the ability to determine elementary resolved layer thicknesses and H retention measurements by depth analysis of LIBS on PFCs exposed in W7-X.

Keywords: laser-induced breakdown spectroscopy, plasma wall interaction, deposition, fuel retention

1. Introduction

Wendelstein 7-X (W7-X) [1] is the largest optimized stellarator in the world and provides a unique platform to study the 3D plasma-wall interaction (PWI) processes [2,3]. These studies include material erosion, transport, deposition and mixing (full material migration cycle) as well as fuel retention by implantation and co-deposition in and on plasma-facing components (PFCs) such as divertor target plates, heat shields and baffles. Elemental analysis with spatial and depth resolution has become a necessary tool for the PFCs research. Several post-mortem methods, such as nuclear reaction analysis (NRA) [4], secondary ion mass spectroscopy (SIMS) [5], thermal desorption spectrometry (TDS) [6] etc., have been used for the *ex situ* material analysis for PWI study. However, post-mortem analysis cannot provide the real-time elemental information of PFCs, especially during the long-pulse discharge operation. It will be more difficult or even inhibited in the future fusion device due to the actively cooled structures of PFCs [7].

Laser-induced breakdown spectroscopy (LIBS) is a well-established elemental analysis approach [8,9]. Its excellent capability has been well demonstrated not only in the lab [10–14] but also in fusion devices such as EAST [15] and TEXTOR [16] for *in situ* studies. However, here we focus on the *ex situ* studies as no system is yet installed in W7-X. Graphite limiter tiles from the initial operational phase in limiter configuration (OP1.1) of W7-X has been carried out by post-mortem analysis of LIBS. The erosion zone and the deposition zone has been measured along the toroidal direction of limiter [17]. It shows that the hydrogen (H) retention content in the deposition dominated zone is higher than in the other zones. The passively cooled graphite divertor has been used in W7-X since OP1.2a campaign in 2016 [1]. Carbon (C) deposition is accompanied by co-deposition with the plasma fuel – H in this case [18]. Therefore the LIBS elemental depth analysis, especially for C and H, is very essential for the PWI study in W7-X.

In this work, LIBS with ps pulse laser is employed to investigate the screws from the baffle region of a divertor module of W7-X. The screws have a multilayer structure with a certain thickness of C layer on the top surface to protect the plasma from potential metallic influx due to the used titanium (Ti) - zirconium (Zr) - molybdenum (Mo) alloy (TZM) material. This structure provides a unique sample to determine the erosion and deposition as well as fuel retention in C layers in W7-X. The linear correlation approach is applied to improve the elemental depth profiles and identify the interface between two layers. The LIBS ablation rate is achieved by using the correlation between the LIBS result and the C layer thickness which has been measured by focused ion beam (FIB) cutting. In addition, H retention intensities on the surface of the new screws and exposed screws are also investigated.

2. Experiment

2.1 Laboratory setup

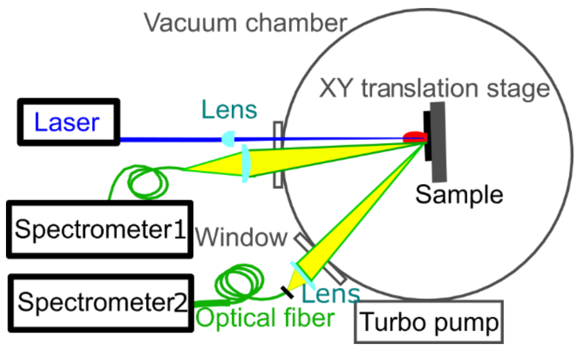

Fig. 1. Schematic of ps LIBS setup with the vacuum chamber for W7-X screws measurement.

The schematic of the LIBS system in the lab is illustrated in Fig. 1. The detail of the optical system can be found in our previous works [17]. A ps pulsed Q-switched laser (PL2241, EKSPLA) at a third harmonic wavelength of 355 nm was used to ablate the target with laser spot size of 0.7 mm diameter and produce the LIBS plasma in a vacuum chamber with a background pressure of 10^{-5} Pa. The laser energy density of 6.5 J/cm^2 was achieved by using the laser energy of 25 mJ/shot. In contrast to previous experiments, besides an overview spectrometer with a wavelength from 350 to 800 nm (HR2000, Ocean Optics), a high-resolution spectrometer in Littrow arrangement with a grating of 1200 lines/mm and a wavelength range of 15 nm combined an ICCD camera (iStar 334, Andor) was also used. The light collection angle was set to 80° or 45° to the surface of the sample. Simultaneously, a quadrupole mass spectrometer could be carried out to quantitatively analyze the H retention on the sample by the laser-induced ablation-quadrupole mass spectrometry (LIA-QMS) approach [19].

2.2 Screw samples

The M6 PFCs were widely installed in the W7-X plasma vessel to fix the graphite tiles for divertor baffles, heat shield and toroidal closures in OP1.2a [20]. The screws have a specific multilayer structure on the TZM substrate which is shown in fig. 2. The protective C layer with different thicknesses on the top surface of the screw was made by magnetron sputtering. This layer was used to protect the metal sputtering from the substrate of the screw and avoid metal impurity production during the discharge plasma exposure, because the graphite divertors have been used in W7-X since OP1.2a campaign. Between the C layer and the TZM substrate, a Ti layer with a thickness of about 1 μm was embedded. In this work, four new screws with C layer thickness between 5.8 μm to 12.0 μm without plasma exposure, and two exposed screws named #14 and #34 which were exposed to about 60 min of H or He plasma operation in W7-X were investigated. The locations of two exposed screws are shown in fig. 3. The #14 screw and #34 screw were located at the inboard side baffle (6v) and outboard side baffle (8h) of lower divertor at module 1, respectively.

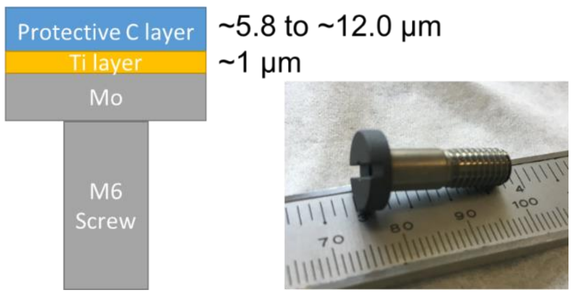

Fig. 2. Schematic and photo of the W7-X screw. The substrate of the M6 screw was TZM. Protective C layer with a thickness of about 5.8 μm to 12.0 μm on the top surface of the screws was made by magnetron sputtering. Between the C and TZM substrate, there was a Ti layer with a thickness of about 1 μm.

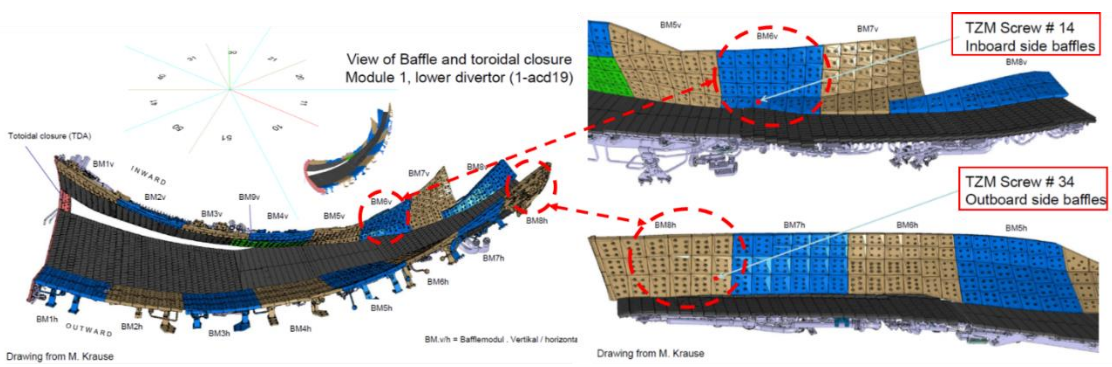

Fig. 3. Locations of exposed screw #14 at the inboard side baffle and exposed screw #34 at outboard side baffle of lower divertor at module 1 in OP1.2a of W7-X.

Fig. 4 shows a typical cross-sectional scanning electron microscopy (SEM) image by FIB cutting on the top surface of two screws. The accuracy thickness of C layer can be clearly determined. The C layer thicknesses of 4 measured new screws are 5.83 μm, 6.96 μm, 9.31 μm and 11.25 μm, respectively. The C layer thicknesses of #14 screw and #34 screw are 11.81 μm and 7.75 μm, respectively.

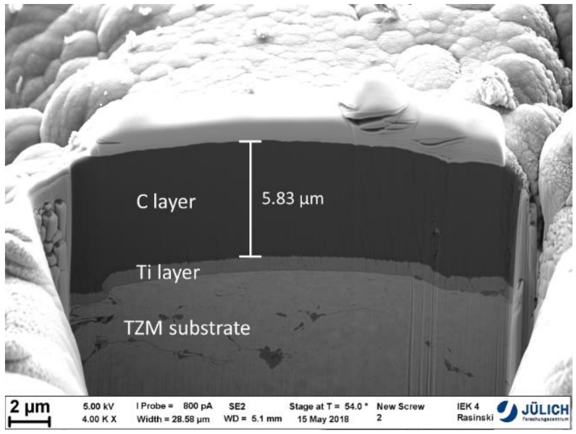

Fig. 4. Typical cross-sectional SEM image on the new screws with C thickness of 5.83 μm (platinum material was coated on the top to protect the surface during the FIB cutting).

3. Results

3.1 LIBS spectra

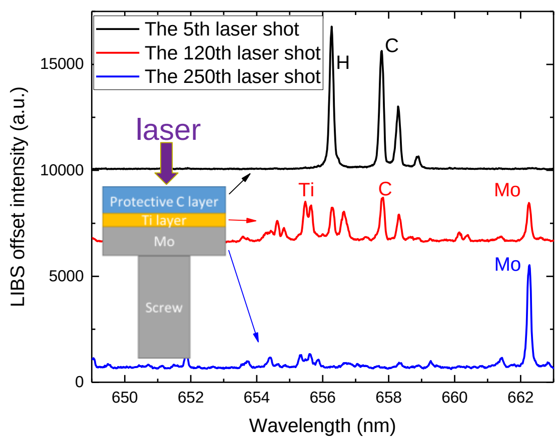

Fig. 5. Typical LIBS spectra with the different number of laser shots to show the characteristic spectral peaks in C layer, Ti layer and Mo substrate of a new screw (C layer thickness of 9.31 μm).

The LIBS spectra are recorded for successive laser shots at the same position on the surface of each screw to obtain the depth profile analysis. The 5th, 120th and 250th spectra are the typical LIBS spectra from the C layer, Ti layer and Mo substrate in the new screw with C layer thickness of 9.31 μm and shown in fig. 5. The H and C spectral peaks are found from LIBS spectrum in the C layer. Because the energy profile of laser is Gaussian and not perfectly rectangular, the Ti signal always accompanies by the C signal and Mo signal in the LIBS spectrum from the Ti layer. Strong Mo signal is found from the LIBS spectrum in the TZM substrate. Because most of the W7-X discharges was using H_2, the He content on the screw is lower than the limit of detection of the LIBS system.

3.2 LIBS elemental depth profile

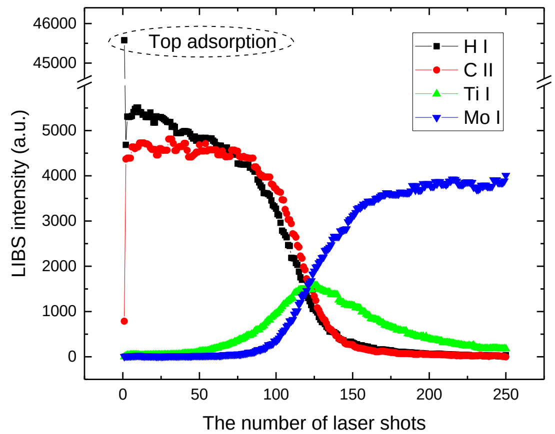

Fig. 6. LIBS elemental depth profiles of Ti I (655.6 nm), H I (656.3 nm), C II (657.8 nm) and Mo I (661.9 nm) intensities on the new screw with C thickness of 9.31 μm.

Elemental depth profiles results can provide the erosion and deposition information about the PFCs. The typical LIBS elemental depth profiles of Ti I (655.6 nm), H I (656.3 nm), C II (657.8 nm) and Mo I (661.9 nm) on the new screw with C thickness of 9.31 μm are shown in fig. 6. The H signal intensity is very high at the top surface of the new screw due to the adsorption of the water from the atmosphere. Subsequently, the H and C intensities behaviors are similar and decrease with depth, thus the H was embedded in the C layer during the deposition process of the layer induced by magnetron sputtering. The Ti layer is the interface layer between the C layer and the Mo substrate, so the Ti intensity increases and then decreases with depth. When the Ti intensity reaches the maximum value, there are also C and Mo signals due to the influence of the energy profile of laser. The Mo intensity from the substrate increases and then plateaus with the depth.

3.3 Residual C layer thickness measurement by LIBS

The measurement and determination of C layer thickness on screws by LIBS are important goals of this work. Thereby, the C layer might be thinner and represent the residual layer in the case the screw was in a net erosion zone or it might be thicker and an additional C layer by plasma deposition is on top of the artificial protection layer. Thus, the local erosion/deposition balance can be studied here in a kind of marker layer approach.

It will be very useful for the on-line and real-time analysis of erosion and deposition on PFCs in the fusion device by an *in situ* LIBS system. The distinction of C layer and Ti layer is very important to measure the thickness information about the C layer. However, due to the Gaussian laser energy profile, it is difficult to accurately determine the interface between C layer and Ti layer in the screw only by using the elemental intensity profiles which are shown in Fig. 6.

Here, a linear correlation approach [21,22] is carried out to obtain the LIBS depth profiles and distinguish the different layers. The linear correlation measures the degree of interrelation between two variables, *x* and *y*, through the linear correlation coefficient, *r*, calculated using the following formula:

$$r = \frac{\sum_i (x_i - \bar{x})(y_i - \bar{y})}{\sqrt{\sum_i (x_i - \bar{x})^2}\sqrt{\sum_i (y_i - \bar{y})^2}}$$

where *x* and *y* are two data sets, $\bar{x}$ is the mean of all x_i, and $\bar{y}$ is the mean of all y_i. The value of *r* lies between −1 and +1, which can be used to indicate the correlation intensity between *x* and *y*. An *r*-value with near to 1 corresponds to complete positive correlation, when *x* and *y* spectra are from the very similar elements. If the *r*-value is near zero, then the *x* and *y* are uncorrelated.

Depth profiles with linear correlation are finally obtained by plotting the evolution of the linear correlation coefficient value for the three reference spectra from the C layer, the Ti layer and the Mo substrate along the depth sequence of spectra. The spectral regions between 649 and 663 nm are selected for the calculation of the linear correlation coefficient. The reference spectra are obtained independently for each screw. The reference spectrum for the C layer is the average spectrum from the 3rd to the 7th depth sequence spectra to avoid the influence of H intensity on the surface. The reference spectrum for the Ti layer is the average spectrum from five spectra around the spectrum which has the maximum Ti LIBS intensity. The reference spectrum for the Mo substrate is the average spectrum from the 246th to the 250th depth sequence spectra. Then, the linear correlated depth profiles are shown in fig. 7. On the first 1 or 2 laser shots, the correlation coefficients for the C layer are low because the very high H intensities are obtained on the surface of the screws. Then, from the third spectra, the correlation coefficients for the C layer are very near to 1 which indicates that the LIBS spectra are from the C layer. Then, with the depth increasing, the correlation coefficients for the C layer decreases and the correlation coefficients for the Ti layer increases. The crossing point means that the spectra from this depth are more correlated to the Ti layer than to the C layer. So the interface between the C layer and the Ti layer can be clearly identified and shown as dotted lines in fig. 7.

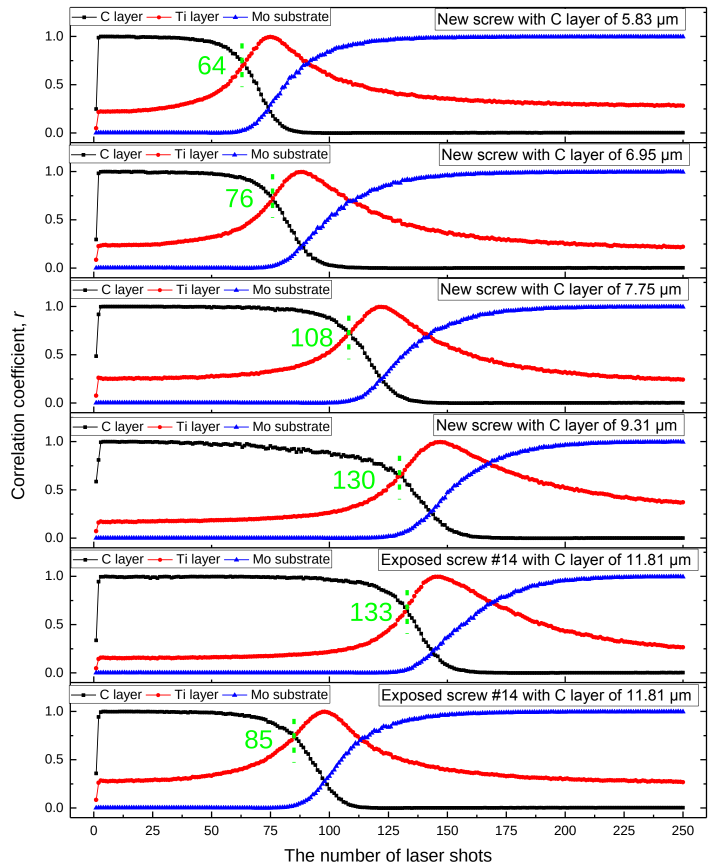

Fig. 7. Correlated depth profiles for the C layer, the Ti layer and the Mo substrate on four new screws and two exposed screws. The dotted lines show the location of the interface between the C layer and the Ti layer.

The correlation between the number of laser shot reaching on the interface between the C layer and the Ti layer and the C layer thickness which is measured by FIB cutting is shown in fig. 8. The results can be well linearly fitted and show that LIBS ablation rate is accurately calibrated. The ablation rate of (82.9 ± 0.9) nm/shot is achieved by a laser energy density of 6.5 J/cm^2. These indicate that the LIBS depth analysis with linear correlation approach can accurately measure the C thickness on the PFCs.

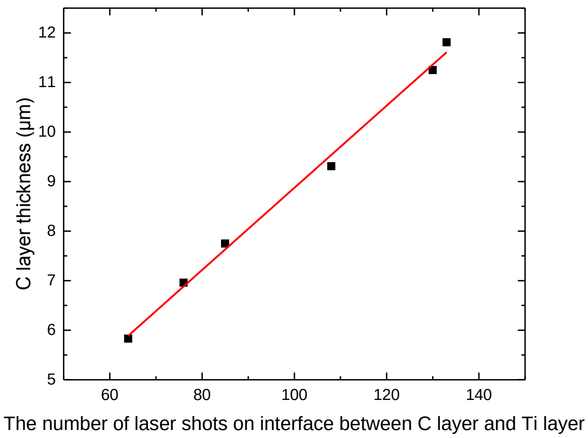

Fig. 8. Correlation of the number of laser shots reach on the interface between the C layer and the Ti layer and the C layer thickness which is measured by FIB. The ablation rate of (82.9 ± 0.9) nm/shot can be achieved.

3.4 H content deposition layer on screw surface

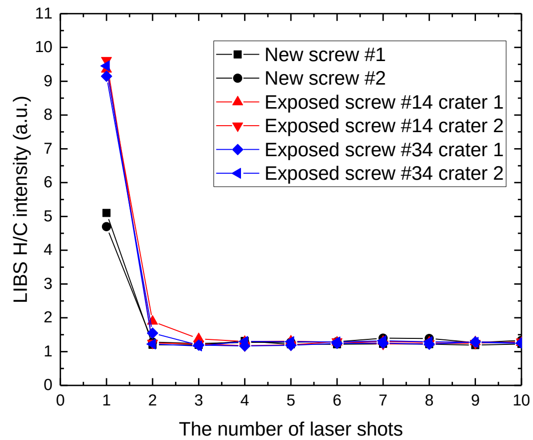

Fig. 9. The depth profiles of the LIBS intensity ratio of H and C on the surface of the new screws and exposed screws.

The H intensity measurement is very important for the study of fuel retention. In order to reduce the influence of laser energy fluctuation, the depth profiles of the LIBS intensity ratio of H and C on the surface of different screws are shown in fig. 9. The H intensities on the surface of exposed screws are higher than on the surface of the new screw without plasma exposure. From the third laser shot, intensities ratio of H and C are almost same for all screws. The SEM photos on the surface of the new screw and exposed screw #14 are shown in fig. 10. Compare to the new screw surface, the deposition layer is found locally on the surface of exposed screws during the plasma exposure in the W7-X, because the screws were recessed to the surrounding baffle graphite surface and located in net deposition zones. The a-C:H layer is rich in H and results in that the LIBS intensity of H on the surface of the exposed screw is higher. In addition, the O content is below the limit of detection, thus not too much O is co-deposited at this location.

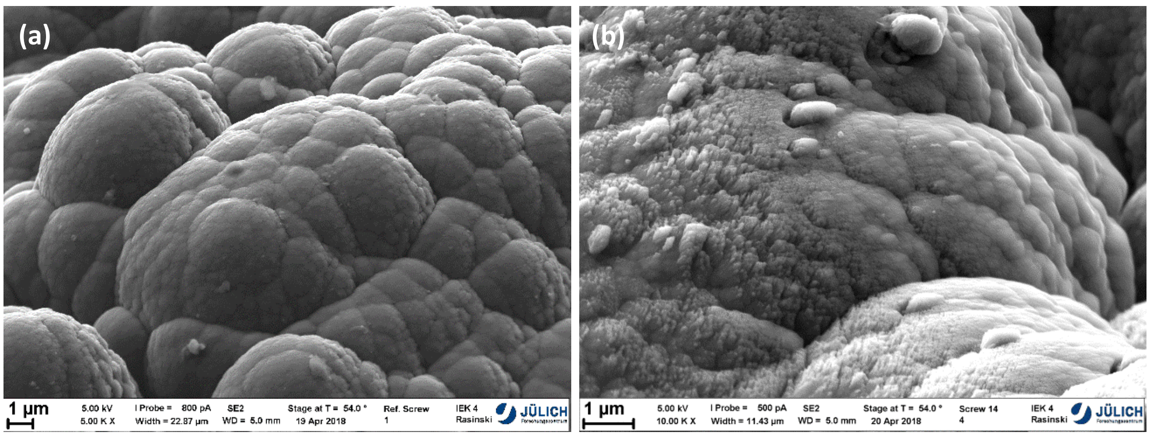

Fig. 10. The SEM photos on (a) the surface of the new screw without plasma exposure and (b) the surface of the exposed screw #14.

4. Conclusion

The ps LIBS method is employed to investigate the elemental depth distribution of screws from the divertor baffle of W7-X in OP1.2a. The screws have a multilayer structure with a certain thickness of C layer from 5.8 μm to 12.0 μm on the top surface. This structure provides a unique sample to determine the erosion and deposition as well as fuel retention on C layer. LIBS depth analysis clearly shows the different behaviors of H, C, Ti and Mo intensities with depth. The H on the surface has very strong intensity due to the surface adsorption. From the third laser shot, the C depth profile and the H depth profile are consistent. The Ti intensities from the interface layer are increases and then decreases with depth. The Mo intensity from the TZM substrate increases and then plateaus with depth. The linear correlation approach has been successfully applied for improving the elemental depth profiles and identifying the interface between the C layer and the Ti layer. The results of the FIB thickness and the LIBS are well fitted and result in that the LIBS ablation rate of (82.9 ± 0.9) nm/shot can be achieved. The erosion and deposition are able to be obtained comparing the thicknesses which are measured before and after the plasma exposure. In addition, LIBS intensities from H retention on the surface of the screws which were exposed to stellarator discharge plasma in OP1.2a are higher than on the surface of the new screw without plasma exposure. The SEM result shows that the high H intensity is due to the plasma deposited a-C:H layer which is found locally on the surface of exposed screws. These indicate that the two exposed screws were located at the net deposition zones at the inboard and outboard side baffles. The studies well demonstrate the ability for the thickness and H retention measurement by depth profile analysis of LIBS on the W7-X divertor baffle screws. This would help us to develop *in situ* LIBS system to monitor the elemental distribution for the 3D PWI study on the divertor of W7-X in further operation phases.

Acknowledgments

This work was supported by the National Science Foundation of China (Nos. 11605023, 11475039), the National Magnetic Confinement Fusion Science Program of China (No. 2013GB109005), China Postdoctoral Science Foundation (Nos. 2017T100172, 2016M591423). This work has been carried out within the framework of the EUROfusion Consortium and has received funding from the Euratom research and training programme 2014-2018 under grant agreement No 633053. The views and opinions expressed herein do not necessarily reflect those of the European Commission.

References

[1] H.-S. Bosch, et al., Final integration, commissioning and start of the Wendelstein 7-X stellarator operation, Nucl. Fusion 57 (2017) 116015.

[2] Y. Liang, et al., Diagnostic set-up and modelling for investigation of synergy between 3D edge physics and plasma-wall interactions on Wendelstein 7-X, Nucl. Fusion 57 (2017) 066049.

[3] S. Brezinsek, Plasma-Surface Interaction and Plasma-Edge Studies in Wendelstein 7-X with Passively Cooled Graphite Divertor, Presented at EPS 45th Conference on Plasma Physics 2018 (Prague).

[4] K. Sugiyama, et al., Ion beam analysis of H and D retention in the near surface layers of JT-60U plasma facing wall tiles, J. Nucl. Mater. 363-365 (2007) 949–954.

[5] M. Mayer, et al. Carbon erosion and deposition on the ASDEX Upgrade divertor tiles, J. Nucl. Mater. 337-339 (2005) 119–123.

[6] T. Shibahara, et al. Hydrogen retention of JT-60 open divertor tiles exposed to HH discharges, Nucl. Fusion 46 (2006) 841–847.

[7] M. Zlobinski, et al., Laser induced desorption as tritium retention diagnostic method in ITER, Fusion Eng. Des. 86 (2011) 1332–1335.
[8] V. Philipps, et al., Development of laser-based techniques for in situ characterization of the first wall in ITER and future fusion devices, Nucl. Fusion 53 (2013) 093002.
[9] C. Li, et al., Review of LIBS application in nuclear fusion technology, Front. Phys. 11 (2016) 114214.
[10] C. Li, et al., Characterization of deuterium retention and co-deposition of fuel with lithium on the divertor tile of EAST using laser induced breakdown spectroscopy, J. Nucl. Mater. 463 (2015) 915–918.
[11] A. Semerok, et al., Laser induced breakdown spectroscopy application in joint European torus, Spectrochim. Acta Part B 123, 121–128 (2016).
[12] J. Karhunen, et al., Applicability of LIBS for in situ monitoring of deposition and retention on the ITER-like wall of JET – comparison to SIMS, J. Nucl. Mater. 463 (2015) 931–935.
[13] P. Paris, et al., Development of laser induced breakdown spectroscopy for studying erosion, deposition, and fuel retention in ASDEX upgrade, Fusion Eng. Des. 98–99 (2015) 1349–1352.
[14] M. Suchonova, et al., Determination of deuterium depth profiles in fusion-relevant wall materials by nanosecond LIBS, Nuclear Mater. Energy, 12 (2017) 611–616.
[15] D. Zhao, et al., Remote in situ laser-induced breakdown spectroscopic approach for diagnosis of the plasma facing components on experimental advanced superconducting tokamak, Rev. Sci. Instrum. 89 (2018) 073501.
[16] Q. Xiao, et al., In-situ analysis of the first wall by laser-induced breakdown spectroscopy in the TEXTOR tokamak: Dependence on the magnetic field strength, J. Nucl. Mater. 463 (2015) 911–914.
[17] C. Li, et al., Laser-induced breakdown spectroscopy for Wendelstein 7-X stellarator limiter tile analysis, Phys. Scr., T170 (2017) 014004.
[18] S. Brezinsek et al., Fuel retention studies with the ITER-Like Wall in JET, Nucl. Fusion 53 (2013) 083023.
[19] J. Oelmann, et al., Depth-resolved sample composition analysis using laser-induced ablation-quadrupole mass spectrometry and laser-induced breakdown spectroscopy, Spectrochim. Acta Part B 144 (2018) 38–45.
[20] C.P. Dhard, et al., Preparation of erosion and deposition investigations on plasma facing components in Wendelstein 7-X, Phys. Scr T170 (2017) 014010.
[21] J. Anzano, et al., Laser-induced plasma spectroscopy for plastic identification, Polym. Eng. Sci. 40 (2000) 2423–2429.

[22] G. Galbacs, et al., Semi-quantitative analysis of binary alloys using laser-induced breakdown spectroscopy and a new calibration approach based on linear correlation, Spectrochim. Acta Part B 56 (2001) 1159–1173.